

Supporting Information

A High-efficiency Blue-LED-excitable Broadband Cr³⁺/Ni²⁺ Co-doped Garnet Phosphor toward Next-generation Spectroscopy Application

Lucheng Liu^{a,b,c}, Yuanhong Liu^b, Tongyu Gao^b, Guantong Chen^b, Ronghui Liu^{b,c,} and*

Xiaodong Li^{a,}*

*Corresponding author

Ronghui Liu

National Engineering Research Center for Rare Earth

E-mail: liuronghui@grirem.com

Xiaodong Li

Northeastern University

E-mail: xdli@mail.neu.edu.cn

a. Key Laboratory for Anisotropy and Texture of Materials (Ministry of Education), School of Materials Science and Engineering, Northeastern University, Shenyang, 110819, P. R. China

b. National Engineering Research Center for Rare Earth, Grirem Advanced Materials Co., Ltd., Beijing 100088, P. R. China

c. General Research Institute for Nonferrous Metals, Beijing 100088, P. R. China

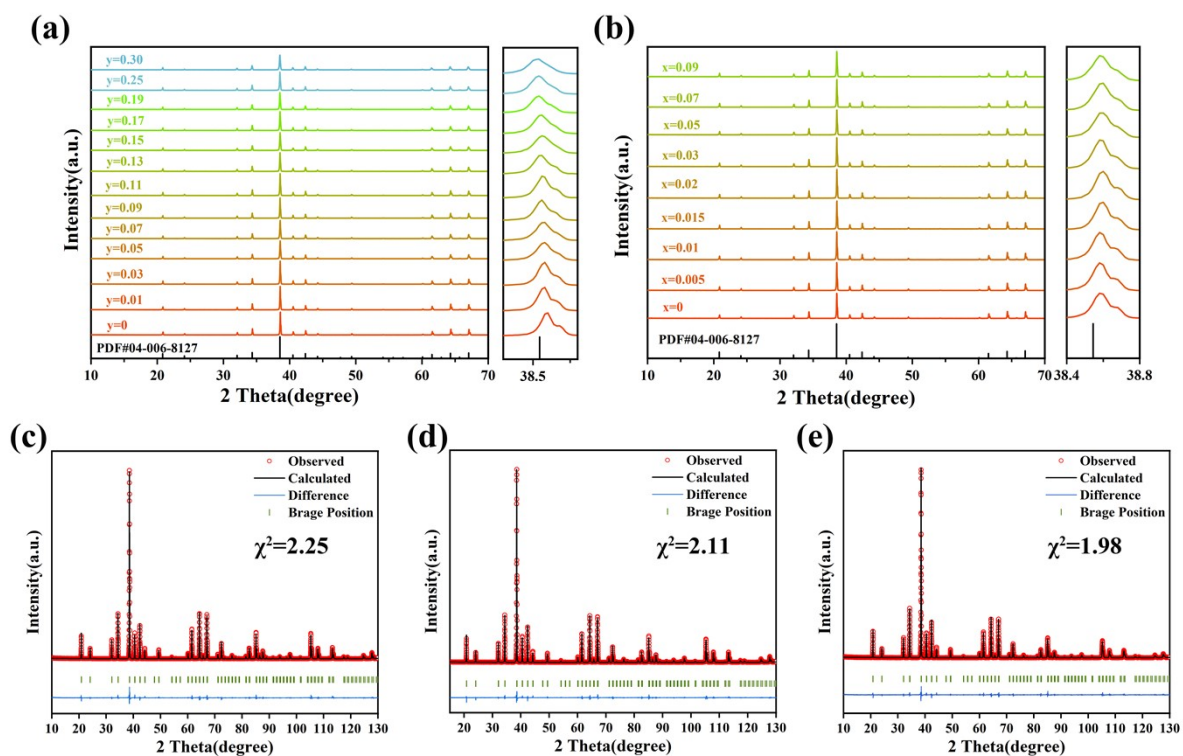


Figure S1. XRD patterns of a) CAGG: $x\text{Cr}^{3+}$, 0.01Ni^{2+} ($0 \leq x \leq 0.30$) and b) CAGG: $y\text{Ni}^{2+}$ ($0 \leq y \leq 0.09$). Rietveld refinement of c) CAGG, d) CAGG: 0.01Ni^{2+} and e) CAGG: 0.15Cr^{3+} .

Table S1. Main parameters of Rietveld refinement of CAGG, CAGG: 0.01Ni^{2+} , CAGG: 0.05Cr^{3+} and CAGG: 0.15Cr^{3+} , 0.01Ni^{2+} samples.

Compound	CAGG	CAGG: 0.01Ni^{2+}	CAGG: 0.15Cr^{3+}	CAGG: 0.15Cr^{3+} , 0.01Ni^{2+}
Space Group	<i>Ia-3d</i>	<i>Ia-3d</i>	<i>Ia-3d</i>	<i>Ia-3d</i>
Symmetry	Cubic	Cubic	Cubic	Cubic
$a = b = c$ (Å)	12.1192(1)	12.1200(1)	12.1272(1)	12.1283(1)
$\alpha = \beta = \gamma$ (°)	90.00	90.00	90.00	90.00
V (Å ³)	1780.01(3)	1780.34(4)	1783.54(4)	1784.01(4)
Al-O(Å)	1.9153	1.9209	1.9187	1.9222
R_p (%)	9.71	9.48	9.02	8.87
R_{wp} (%)	14.8	14.9	14.6	14.5
R_{exp} (%)	9.98	10.24	10.34	9.97
χ^2	2.25	2.11	1.98	2.13

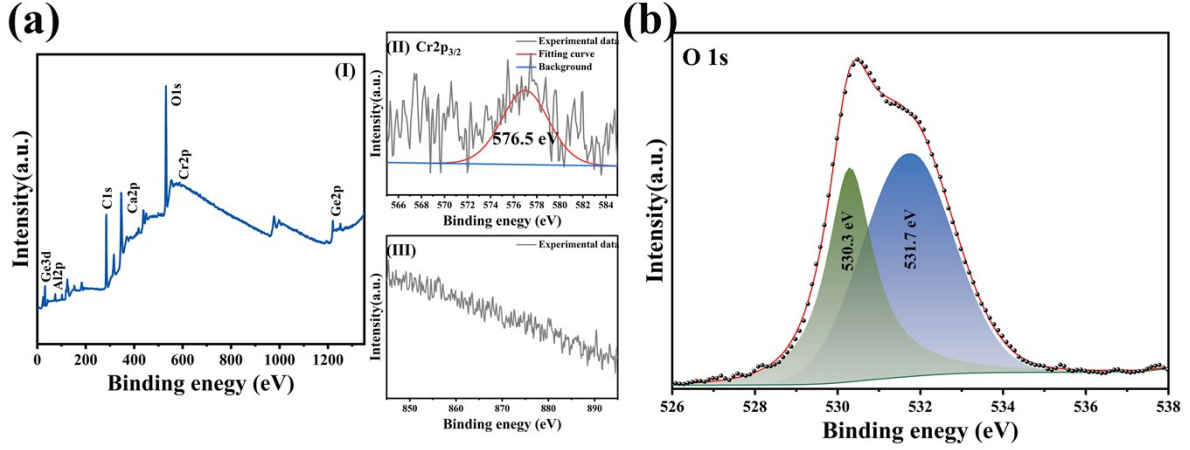


Figure S2. a) (I) XPS full spectrum for CAGG:0.15Cr³⁺,0.01Ni²⁺, (II) XPS: Cr 2p spectrum and (III) XPS: Ni 2p spectrum. b) XPS: O 1s spectrum.

According to Kubelka-Munk function, the band gap energy (E_g) can be estimated using the following formulas (S1) and (S2):¹

$$[F(R)hv]^n = A(hv - E_g) \quad \backslash * \text{MERGEFORMAT (S1)}$$

$$F(R) = \frac{(1 - R)^2}{2R} \quad \backslash * \text{MERGEFORMAT (S2)}$$

where R , $F(R)$, $h\nu$, and A stand for relative reflectance, K-M function, specific phonon energy, and scale factor, respectively. And $n = 2$ for direct transition or $n = 1/2$ for indirect transition. This band structure of CAGG matrix is direct, and $n = 2$. The optical bandgap E_g can be determined by extrapolating the straight part of $[h\nu F(R)]^2$ to the $h\nu$ plot associated with the energy axis.

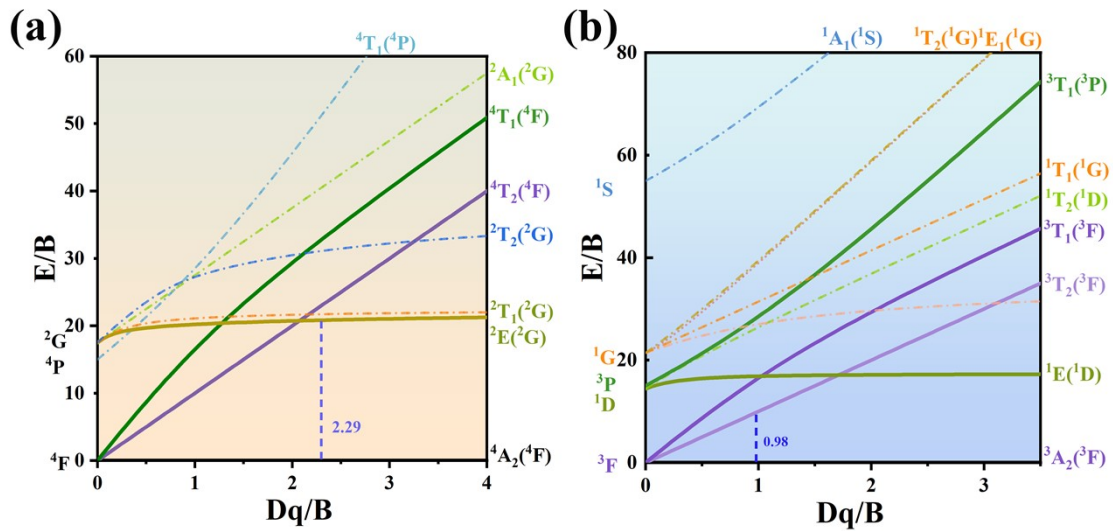


Figure S3. The T-S energy level diagram of a) $3d^3$ and b) $3d^8$ configuration in octahedral crystal field.

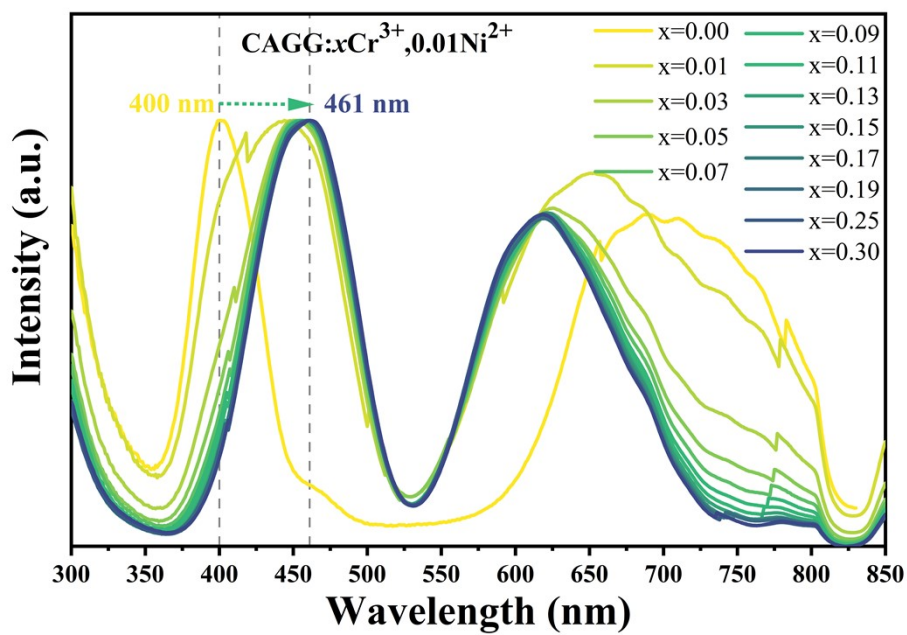


Figure S4. The normalized excitation spectra of $\text{CAGG}:x\text{Cr}^{3+}, 0.01\text{Ni}^{2+}$ monitored at 1423 nm.

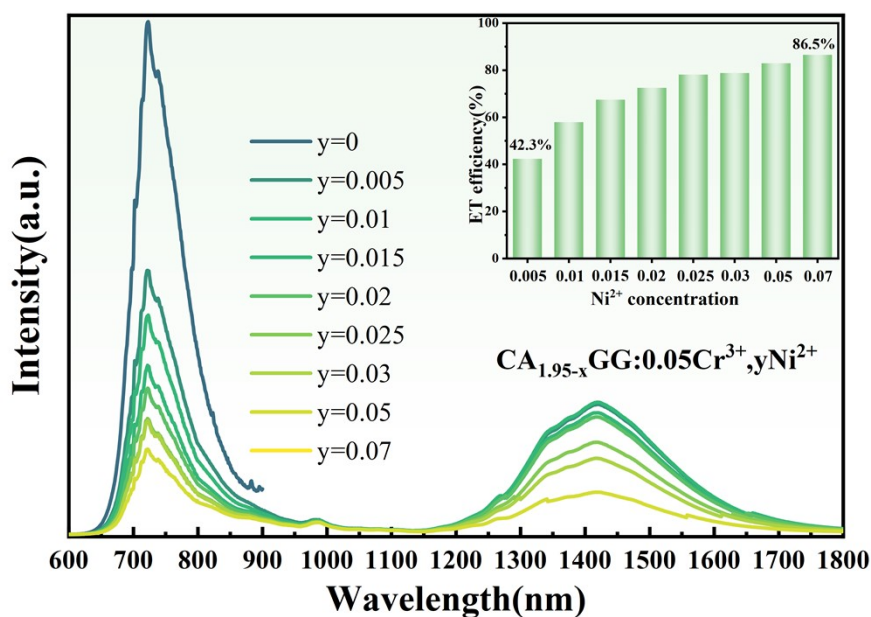


Figure S5. The emission spectra of $\text{CAGG}:0.05\text{Cr}^{3+}, y\text{Ni}^{2+}$ ($y=0\sim 0.09$) under 460 nm excitation.

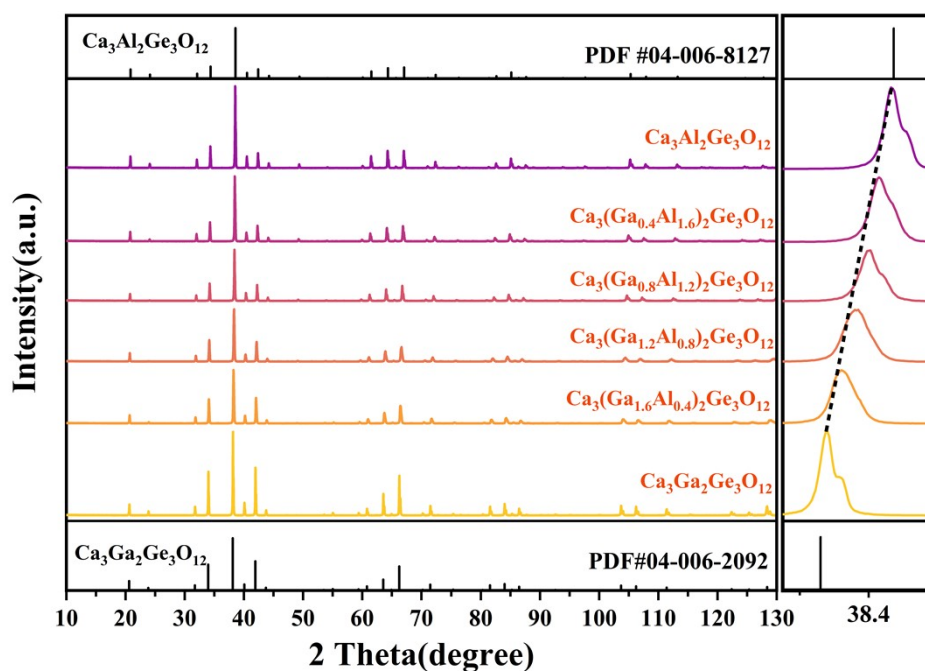


Figure S6. The XRD patterns of the $\text{Ca}_3(\text{Ga}_{1-z}\text{Al}_z)_2\text{Ge}_3\text{O}_{12}:0.05\text{Cr}^{3+}$ ($z=0-1$) samples

Table S2. Main parameters of rietveld refinement of $\text{Ca}_3(\text{Ga}_{1-z}\text{Al}_z)_2\text{Ge}_3\text{O}_{12}:0.05\text{Cr}^{3+}$ samples.

Compound	Z=0	Z=0.4	Z=0.8	Z=1.2	Z=1.6	Z=2.0
Space Group	<i>Ia-3d</i>	<i>Ia-3d</i>	<i>Ia-3d</i>	<i>Ia-3d</i>	<i>Ia-3d</i>	<i>Ia-3d</i>
Symmetry	Cubic	Cubic	Cubic	Cubic	Cubic	Cubic
a (Å)	12.2543(1)	12.2251(1)	12.2002(1)	12.1702(1)	12.1466(1)	12.123(1)
$\alpha = \beta = \gamma$ (°)	90.00	90.00	90.00	90.00	90.00	90.00

V (\AA^3)	1840.21(3)	1827.10(4)	1815.95(4)	1802.61(4)	1792.10(4)	1781.68(4)
Ga/Al-O(\AA)	1.9896	1.9787	1.9584	1.9400	1.9290	1.9151
R_p (%)	8.39	9.34	9.00	9.99	9.49	11.00
R_{wp} (%)	13.5	14.4	13.7	15.0	14.5	15.6
R_{exp} (%)	9.14	10.15	10.28	11.25	10.43	10.36
χ^2	2.18	2.02	1.77	1.79	1.92	2.26

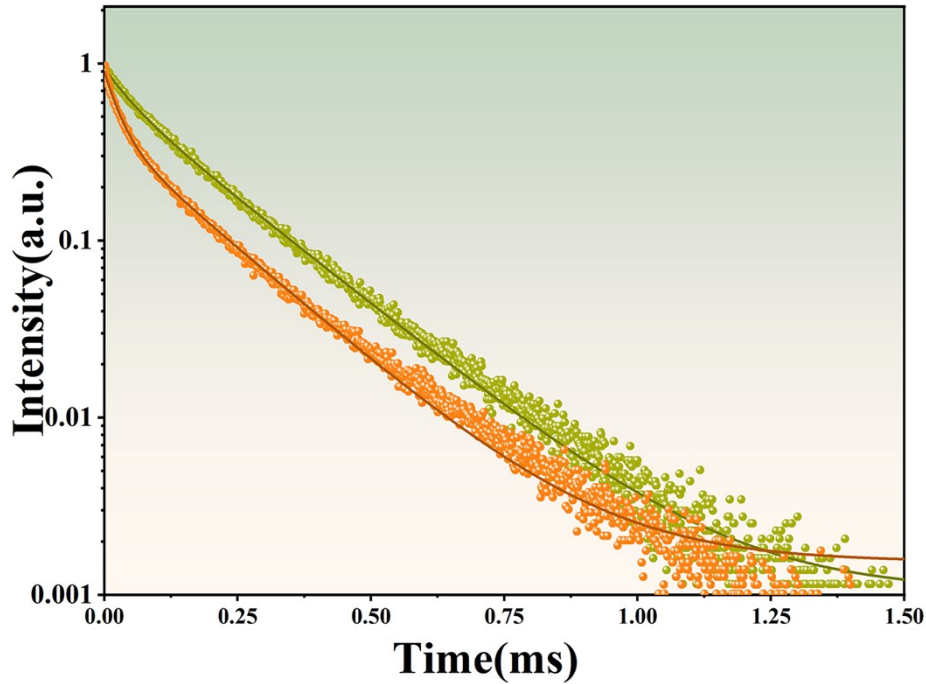


Figure S7. Lifetime and fitting curve of CAGG:0.15Cr³⁺ and CAGG: 0.15Cr³⁺, 0.01Ni²⁺

The fluorescence decay curves of CAGG:0.15Cr³⁺, y Ni²⁺ ($y=0, 0.01$) can be well-fitted by a double exponential function: [2]

$$I(t) = I_0 + A_1 e^{-\frac{t}{\tau_1}} + A_2 e^{-\frac{t}{\tau_2}} \quad \backslash * \text{MERGEFORMAT (S3)}$$

Where $I(t)$ represent the luminescence intensity as a function of time t . I_0 represents the original intensity, A_1 and A_2 are constants. τ_1 and τ_2 are the two components of the decay time. The average lifetime and ET efficiency can be calculated by the following equation: [2]

$$\tau_{ave} = \frac{A_1 \tau_1^2 + A_2 \tau_2^2}{A_1 \tau_1 + A_2 \tau_2} \quad \backslash * \text{MERGEFORMAT (S4)}$$

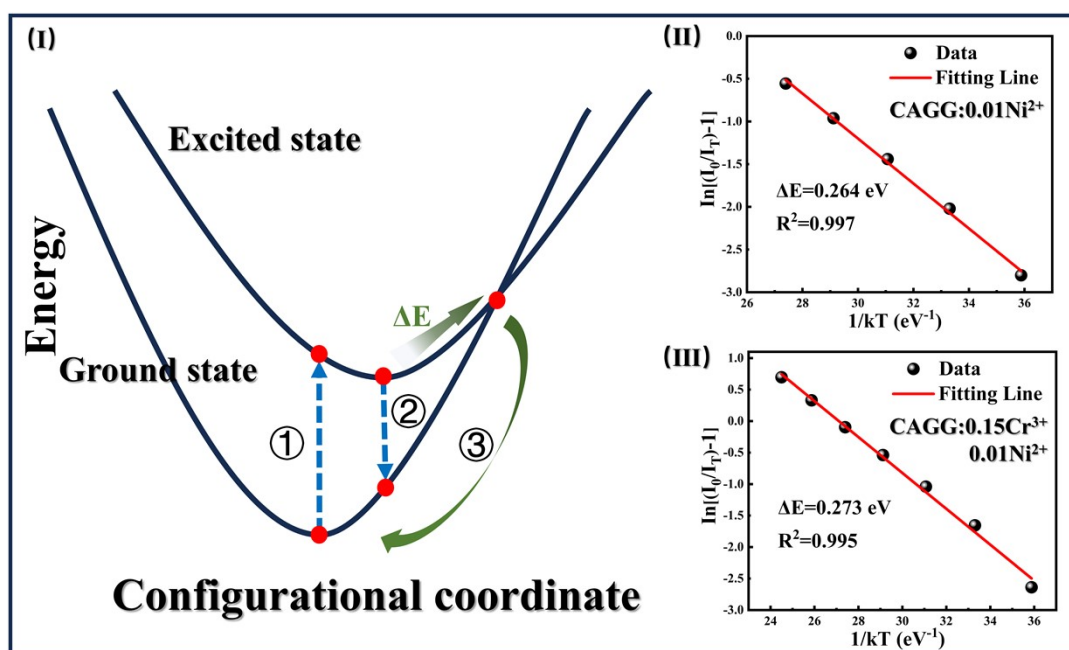


Figure S8. (I) Configurational coordinate diagram to illustrate thermal quenching behavior. The fitting results of the thermal activation energy to (II)CAGG:0.01Ni²⁺ and (III) CAGG:0.15Cr³⁺,0.01Ni²⁺.

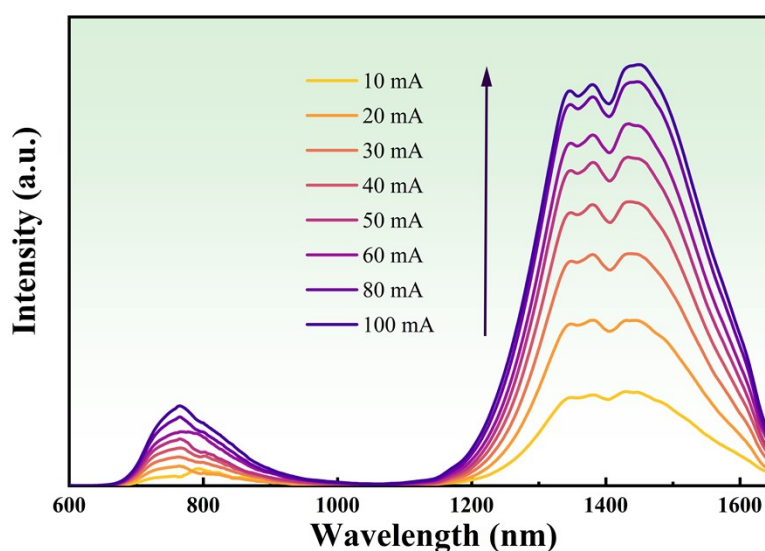


Figure S9. EL spectra of NIR pc-LEDs at different currents

- (1) P. Makuła, M. Pacia, W. Macyk, How To Correctly Determine the Band Gap Energy of Modified Semiconductor Photocatalysts Based on UV-Vis Spectra. *J. Phys. Chem. Lett.* **2018**, 9 (23), 6814. DOI: 10.1021/acs.jpcllett.8b02892.
- (2) Li, J.; Wang, C.; Niu, Y.; Wang, Y.; Wu, F.; Qi, z.; Teng, Y.; Dong, H.; Mu, Z. Efficient

Broad-Band NIR-II Emitting Phosphor $\text{Mg}_4\text{Ta}_2\text{O}_9$: Ni^{2+} with Satisfactory Thermal Stability of Luminescence. *Ceram. Int.* **2024**, *50* (11), 18647-18654. DOI: 10.1016/j.ceramint.2024.02.353.